

Qubit quantum mechanics with correlated-photon experiments

Enrique J. Galvez

Department of Physics and Astronomy, Colgate University, Hamilton, New York 13346

(Received 8 October 2009; accepted 7 February 2010)

A matrix-based formalism is used to explain the results of undergraduate level quantum mechanics experiments with correlated photons. The article includes new variations of experiments and new results. A discussion of our experience with a correlated-photon laboratory component for an undergraduate course on quantum mechanics is presented. © 2010 American Association of Physics Teachers. [DOI: 10.1119/1.3337692]

I. INTRODUCTION

In the past 30 years experiments with correlated photons have brought new understanding of fundamental aspects of quantum mechanics. More recently, the equipment and techniques have become less expensive and simpler so that they may be introduced into the undergraduate laboratory.¹⁻⁵ The significance of the experiments is that they address fundamental questions of quantum mechanics that until recently were not thought to be possible in an undergraduate environment. The rapid increase in the importance of quantum information also calls for a better introduction to quantum mechanics early in the physics curriculum. These experiments help advance this goal with a hands-on approach.

The first place where correlated-photon experiments have been implemented is in semester-long upper-level laboratory projects. These experiments form ideal advanced-laboratory projects because of the size of the setup (fitting on a 2×5 ft² optical breadboard), and the variety of experiments that can be done with the same equipment. Beyond being used as projects, the experiments can be used in a few-week advanced laboratory⁶ or a collection of them in a laboratory component for a quantum mechanics course, as I report here. Other creative initiatives include introducing quantum mechanics and associated laboratories in courses earlier in the curriculum.⁷⁻⁹

The virtue of the experiments is that they confront the nonintuitive predictions of quantum mechanics directly. The availability of these experiments gives us an additional motivation to treat fundamental questions. Another positive aspect of these experiments is that they can be explained by direct application of the algebra of quantum mechanics.

Since 2005 we have offered a suite of experiments as a laboratory component to an introductory course on quantum mechanics at Colgate University.¹⁰ Whitman College¹¹ follows a similar practice, and a larger institution, University of Rochester,¹² incorporates these type of experiments as part of a quantum optics curriculum. Our class size ranges between 9 and 16 students and employs two setups for five separate laboratory experiments. Our choice of experiments has been laboratory basics and Stern–Gerlach-like polarization projections, interference of light in a Mach–Zehnder interferometer and the Hanbury–Brown–Twiss experiment, the quantum eraser, biphoton interference, and entanglement and Bell’s inequalities. In the development phase these experiments served as advanced-laboratory semester-long capstone research projects. Some of these experiments proceeded into research studies.¹³⁻¹⁵

The purpose of this article is to elaborate further on these experiments by proposing a treatment that adapts well to the linear algebra formalism of the course, and discussing new

variations of the experiments. Our course on introductory quantum mechanics, taught to juniors and seniors, covers the Dirac notation and the physics of spins before covering wave-mechanical concepts.¹⁶ The physics of spin-1/2 particles, fundamental to quantum physics, can be explained effectively within the framework of light polarization.¹⁷ The discussion of these fundamental topics arises naturally because they are readily testable in the laboratory component of the course. New texts follow this path of addressing fundamental concepts as part of an introduction to quantum mechanics.¹⁸

In this article we use the matrix formalism and the concept of qubits in correlated-photon experiments and show how we can easily adapt a matrix-based framework to all these experiments. To describe the experiments we use Dirac notation and a particle-labeling format, the notation of choice in quantum computing. We do not use second quantization and the photon number states¹⁹ because these concepts go beyond the scope of an undergraduate quantum mechanics course. The particle-labeling format gives the correct answers provided that when describing identical photon pairs, we use wave functions with the proper symmetry. To describe heralded-photon experiments where one photon goes directly to a detector and the other goes through a quantum-processing apparatus, we simplify the notation by using the wave function of only the photon that goes through the apparatus but keep in mind that a more complete description should use a two-photon wave function.

The possibility of building a quantum processor has led to an entire new approach to logic called quantum logic. This approach is now being introduced to physicists at various levels¹⁸⁻²¹ and to computer scientists and mathematicians.²²⁻²⁴ Because linear optics experiments remain a viable approach for implementing a quantum processor, these correlated-photon experiments are an opportunity to introduce qubit manipulation into quantum mechanics courses.

When discussing two-particle entanglement, the quantum-information community uses a concept, the density matrix, that is mostly ignored in undergraduate quantum physics texts. We advocate that the density matrix should play a more prominent role in quantum mechanics instruction. The importance of this concept is that it can treat entangled states and their classical-realistic counterpart, mixed states, within the same framework. Mixed states are important because they serve as a contrast to the purely quantum mechanical concept of entanglement.

This article is organized as follows. The formalism and associated experiments are divided in terms of the size of the Hilbert space of the corresponding quantum mechanical de-

scription, starting with one qubit (two dimensions), following with two qubits (four dimensions), and ending with a brief discussion of higher dimensional spaces. We present new experimental data in each section to highlight the rich variety of experiments that can be done with the same setup. The mathematical framework is the one we used in conjunction with the laboratory component of our quantum mechanics course, which we found to be appealing due to its consistency throughout the experiments. I finish with a brief description of our experience with the laboratory component and student feedback.

II. SINGLE QUBIT

“It from bit,” a thoughtful expression by Wheeler,²⁵ who forecasted an approach to use quantum states as information. A qubit represents a system in a two-dimensional Hilbert space. For a single photon there are two simple spaces: Polarization and the direction of propagation.

A. Polarization space

The space of states of polarization has been treated extensively, with the usual basis being the eigenstates of linear polarization: Horizontal and vertical. These eigenstates can be represented in vector format as

$$|H\rangle = \begin{pmatrix} 1 \\ 0 \end{pmatrix} \quad (1a)$$

and

$$|V\rangle = \begin{pmatrix} 0 \\ 1 \end{pmatrix}. \quad (1b)$$

Optical elements can be represented by operators acting on the quantum state of photons. This aspect has been treated classically with the Jones matrix formalism (see, for example, Ref. 26), and Jones operators can be expressed in terms of Pauli matrices.²⁷ The most common operators are half and quarter wave plates, given respectively by

$$\hat{W}_{\lambda/2} = \begin{pmatrix} 1 & 0 \\ 0 & -1 \end{pmatrix} \quad (2)$$

and

$$\hat{W}_{\lambda/4} = \begin{pmatrix} 1 & 0 \\ 0 & i \end{pmatrix}. \quad (3)$$

The rotated wave plate is a good example of the use of rotations for either rotated bases or rotated operators. The rotated operator for the half-wave plate is given by

$$\hat{W}_{\lambda/2}(\theta) = \hat{R}(\theta)\hat{W}_{\lambda/2}\hat{R}(-\theta) = \begin{pmatrix} \cos 2\theta & \sin 2\theta \\ \sin 2\theta & -\cos 2\theta \end{pmatrix}, \quad (4)$$

where we have used

$$\hat{R}(\theta) = \begin{pmatrix} \cos \theta & -\sin \theta \\ \sin \theta & \cos \theta \end{pmatrix} \quad (5)$$

as the operator that rotates vectors by the angle θ . If $\theta = \pi/8$, the wave plate has the form of the Hadamard gate, which has special significance for quantum computation.²²⁻²⁴ It transforms the square basis to the diagonal basis. A polarizer with its transmission axis along the H -direction is given by the nonunitary expression

$$\hat{P}_H = \begin{pmatrix} 1 & 0 \\ 0 & 0 \end{pmatrix}. \quad (6)$$

A polarizer projects the state of the light along the horizontal direction: $\hat{P}_H = |H\rangle\langle H|$. A polarizer with transmission axis along the H' direction, which is the H -direction rotated by the angle θ , is given by

$$\hat{P}_{H'} = \begin{pmatrix} \cos^2 \theta & \sin \theta \cos \theta \\ \sin \theta \cos \theta & \sin^2 \theta \end{pmatrix}. \quad (7)$$

The latter can be used for problems mimicking the passage of spins through consecutive Stern–Gerlach apparatuses and understanding the state-changing role of a measuring device such as a polarizer.⁵

B. Direction of propagation

The passage of photons through an interferometer can be explained in terms of operations in the two-dimensional space of propagation directions. A Mach–Zehnder interferometer is the most convenient one to use because it clearly separates the propagation directions of the two paths. Because the directions of propagation in this setup are orthogonal, we can set their eigenstates to be

$$|X\rangle = \begin{pmatrix} 1 \\ 0 \end{pmatrix}, \quad (8a)$$

and

$$|Y\rangle = \begin{pmatrix} 0 \\ 1 \end{pmatrix}, \quad (8b)$$

where the labels X and Y specify the state of the light propagating along orthogonal directions. The optical components of the interferometer can be represented as operators. Thus, the operator for the symmetric non-polarizing beam splitter is

$$\hat{B} = \frac{1}{\sqrt{2}} \begin{pmatrix} 1 & i \\ i & 1 \end{pmatrix}, \quad (9)$$

and the operator for the mirror is

$$\hat{M} = \begin{pmatrix} 0 & 1 \\ 1 & 0 \end{pmatrix}. \quad (10)$$

The mirror acts as a “not” gate for these direction-of-propagation qubits because it flips the two bits. In addition, we must account for the phases due to the passage through the arms of the interferometer. We do this with the operator

$$\hat{A} = \begin{pmatrix} e^{i\delta_1} & 0 \\ 0 & e^{i\delta_2} \end{pmatrix}, \quad (11)$$

where δ_1 and δ_2 are the phases corresponding to the arm lengths ℓ_1 and ℓ_2 , respectively.

The interferometer is represented by the operator

$$\hat{Z} = \hat{B}\hat{A}\hat{M}\hat{B} = 2ie^{i(\delta_1/2+\delta_2/2)} \begin{pmatrix} \cos(\delta/2) & -\sin(\delta/2) \\ \sin(\delta/2) & \cos(\delta/2) \end{pmatrix}, \quad (12)$$

where $\delta = \delta_2 - \delta_1$. Thus, if the light is in the initial state $|\psi_i\rangle$, the final state will be in the state $|\psi_f\rangle = \hat{Z}|\psi_i\rangle$. A measurement at one of the output ports, say, X , constitutes a projection: $\hat{P}_X = |X\rangle\langle X|$. Thus, the probability of a photon exiting the in-

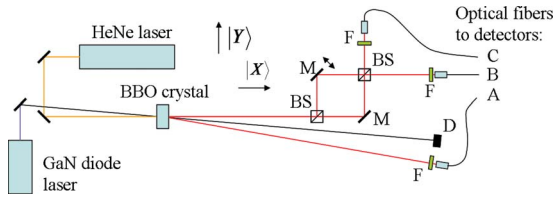


Fig. 1. Standard layout for doing experiments with correlated photons. Interferometer components are nonpolarizing beam splitters (BS) and metallic mirrors (m). Band-pass filters (f) precede couplers to multimode fibers, which send light to detectors A, B, and C. The beam dump (d) collects the pump beam for safety.

interferometer along the X -direction is $\mathcal{P}_X = |\hat{P}_X|\psi_f\rangle|^2$. For example, if $|\psi_i\rangle = |X\rangle$, it is easy to show that $\mathcal{P}_X = \cos^2(\delta/2) = (1/2)(1 + \cos \delta)$. An important point for students to understand is the following. If $\delta = \pi$, the probability is zero. And where does the energy go? The answer is provided by calculating the probability of detecting a photon exiting the interferometer along the Y -direction. In this case $\mathcal{P}_Y = |\hat{P}_Y|\psi_f\rangle|^2 = \sin^2(\delta/2) = (1/2)(1 - \cos \delta)$, that is, if the light does not exit through the X port, it does so through the Y port.

As we have seen, optical components such as mirrors, beam splitters, wave plates, and the entire interferometer can be represented by matrices. They perform the evolution of the state of the light as it propagates. They are unitary but not necessarily Hermitian because they do not perform a measurement. The essence of quantum computing is the processing of quantum states by unitary transformations. Measurements are provided by the detectors and are represented by corresponding projection operators.

The experiments have a standard layout as shown in Fig. 1. Since our previous publication,⁵ we have converged to using gallium nitride (GaN) diode lasers (wavelength of 405 nm and power of 15–50 mW) to produce correlated-photon pairs with a beta-barium-borate nonlinear crystal via type-I spontaneous parametric down-conversion. The layout is designed to produce degenerate pairs leaving the crystal at ± 3 deg. Because we use interferometers, in most of the experiments we employ a helium-neon (HeNe) laser to help with alignment. The setup is designed so that the light paths through the interferometer are parallel to the rows of holes in the optical breadboard. This layout makes the alignment straightforward with the help of an iris.²⁸ The light is sent to a fiber-coupled four-detector module (Perkin Elmer model SPCM-AQ4C) via multimode optical fibers. We use coincidence modules (Camberra model 2040) to record the data. This use is an alternative to the method we reported earlier with time-to-amplitude converters,⁵ but simpler alternatives are available.^{29,30} The use of four detectors greatly enhances the variety of experiments that can be done, as we will discuss. To scan the interferometer phase, we move one of the mirrors, which are mounted on a translation stage. By applying a voltage to a piezoelectric placed as a spacer in the translation stage, we move the mirror and effectively change the phase. The data acquisition program, written in LABVIEW, scans a voltage that is amplified externally by a factor of 15 and applied to the piezoelectric.

The results of single photons going through the interferometer and being detected at the two outputs of the interferometer are shown in Fig. 2. The horizontal scale is proportional to the voltage that is applied to the piezoelectric (V_p),

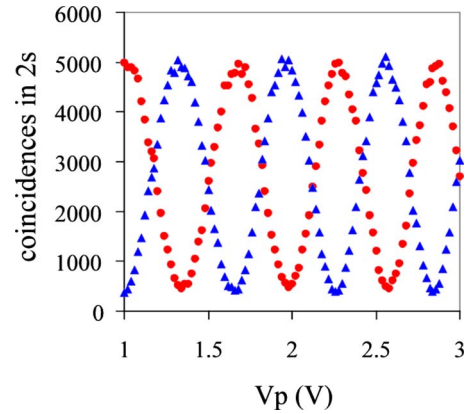


Fig. 2. Single-photon interference obtained with the setup in Fig. 1. Coincidence counts at detectors A and B (circles), and A and C (triangles) represent detections, where heralded photons leave the interferometer along the directions X and Y , respectively.

which pushes one of the mirrors of the interferometer. The data clearly show that the outputs of the interferometer are complementary, consistent with the predictions. The data shown throughout this article are typical of what is expected of a one afternoon laboratory. Nonideal visibilities are typical of the experimental conditions, which include slight misalignments of the apparatus and a lack of better mode matching. A more serious effort, such as would be involved in an advanced laboratory or capstone project, results in data of better quality.

Note that within a global phase, \hat{Z} is a unitary operator that rotates the direction of the propagation basis by the angle $\theta = \delta/2$.²⁷ Thus, an interferometer can be used for unitary operations on direction-of-propagation qubits.

Quantum mechanics provides one of its mysteries when it allows the state $(1/\sqrt{2})(|X\rangle + |Y\rangle)$, which signifies that the quantum of light, the photon, to travel in both directions at once. This situation appears when the light is traveling after the first beam splitter of the interferometer. A remaining topic of debate concerns making explicit references to non-intuitive statements such as the previous one; this statement is equivalent to saying that in a double-slit experiment a photon (or electron, or anything) goes through both slits at once. Alternatively we can say that when the apparatus is set up to detect particle aspects, the photons behave as a whole and do not split, but when the apparatus is setup to detect wave aspects, photons act as waves going through both paths and interfering. The virtue of the photon experiments is that they address these issues and show that the predictions of quantum mechanics are true, as nonintuitive as they may seem. The qubit is the cornerstone of quantum information precisely because of its indefiniteness, that is, a system is 1 and 0 instead of 1 or 0.

III. TWO QUBITS

When a system can be in two two-dimensional Hilbert spaces, it is described by a greater combined Hilbert space. For two qubits the Hilbert space has four dimensions. In this section we analyze the various two-qubit scenarios provided by correlated-photon experiments.

A. One photon in two modes

The quantum eraser is an experiment involving two qubits and a single quantum object, a photon. In this case one mode is provided by the direction of propagation, and the second mode is provided by the polarization. If the general states of each mode are

$$\begin{pmatrix} x \\ y \end{pmatrix} \quad \text{and} \quad \begin{pmatrix} h \\ v \end{pmatrix} \quad (13)$$

for the direction of propagation and polarization modes, respectively, then the two-qubit wave function is given by the tensor or Kronecker product²⁴

$$\begin{pmatrix} x \\ y \end{pmatrix} \otimes \begin{pmatrix} h \\ v \end{pmatrix} = \begin{pmatrix} xh \\ xv \\ yh \\ yv \end{pmatrix}. \quad (14)$$

Eigenstates of this two-qubit system can be represented by the short-hand notation

$$|XH\rangle = \begin{pmatrix} 1 \\ 0 \end{pmatrix} \otimes \begin{pmatrix} 1 \\ 0 \end{pmatrix} = \begin{pmatrix} 1 \\ 0 \\ 0 \\ 0 \end{pmatrix}, \quad (15)$$

and similarly for $|XV\rangle$, $|YH\rangle$, and $|YV\rangle$.

A version of the quantum eraser involves putting a half-wave plate in one of the arms of the interferometer. In actual experiments the other arm has a dummy half-wave plate with its fast axis vertical to equalize the path lengths.⁵ In the first stage of the experiment the fast axis of the wave plate is set to vertical. In this stage the paths of the interferometer are indistinguishable. In the second stage the wave plate is rotated by 45° so that the polarization of the light going through that arm is rotated by 90° . In this case the paths of the interferometer are distinguishable. In the third stage a polarizer, with transmission axis forming 45° with the horizontal, is placed along the X -direction after the interferometer. In this case the path information is erased along the X -direction after the interferometer.

We explain this experiment in the qubit formulation as follows. The input state of the light is state $|XV\rangle$. The interferometer can be described by a matrix, which contains combined polarization and direction-of-propagation matrices. The matrix describing the interferometer is given by

$$\hat{Z}_{dp}(\theta) = (\hat{B} \otimes \hat{I})(\hat{A} \otimes \hat{I})\hat{W}_{\lambda/2}(\theta)(\hat{M} \otimes \hat{I})(\hat{B} \otimes \hat{I}), \quad (16)$$

where \hat{I} is the identity and

$$\hat{W}_{\lambda/2}(\theta) = \begin{pmatrix} \cos 2\theta & \sin 2\theta & 0 & 0 \\ \sin 2\theta & -\cos 2\theta & 0 & 0 \\ 0 & 0 & 1 & 0 \\ 0 & 0 & 0 & -1 \end{pmatrix}. \quad (17)$$

The construction of this matrix is done by hand by noting that a two-qubit 4×4 matrix can be divided into four 2×2 submatrices. The upper left and lower right diagonal submatrices locate the 2×2 polarization matrices, which represent elements along the X - and Y -directions, respectively. In our case they locate the rotatable half-wave plate along the

X -direction of one arm and the dummy half-wave plate in the Y -direction of the other arm. The off-diagonal submatrices are zero because they would mix the polarization components of one direction with those of the other direction, something that a wave plate does not do. A polarizing beam splitter is an example of a device that mixes polarization and direction of propagation, as we will see later.

In the first stage of the experiment, we have $\theta=0$. The output state is

$$\hat{Z}_{dp}(0)|XV\rangle = \frac{i}{2} \begin{pmatrix} 0 \\ -e^{i\delta_1} - e^{i\delta_2} \\ 0 \\ e^{i\delta_1} - e^{i\delta_2} \end{pmatrix}. \quad (18)$$

The terms in the second and fourth rows of Eq. (18) represent interference. Detecting the light along the X -direction implies making a direction-of-propagation projection $\hat{P}_X=|X\rangle\langle X|$. The probability of detecting a photon is $\mathcal{P}_X(0)=|(\hat{P}_X \otimes \hat{I})\hat{Z}_{dp}(0)|XV\rangle|^2=(1/2)(1+\cos \delta)$.

For the second stage the final state is

$$\hat{Z}_{dp}(\pi/4)|XV\rangle = \frac{i}{2} \begin{pmatrix} e^{i\delta_1} \\ -e^{i\delta_2} \\ -e^{i\delta_1} \\ -e^{i\delta_2} \end{pmatrix}. \quad (19)$$

Because the probability of any particular output is the absolute value squared, it is easy to see that Eq. (19) contains no interference terms. It is easy to calculate $\mathcal{P}_X(\pi/4)=1/2$, and hence there is no interference when the paths are distinguishable because the path information is encoded in the polarization. We note that to calculate the probability, we make a partial measurement in the propagation direction basis because we never make a measurement in the polarization basis.

This outcome is typical of quantum mechanics: Interference disappears even if we do not obtain the distinguishing information—all that is necessary is that the path information be available for the interference to disappear. Here it is important to understand the result of experiments that dispel an old belief regarding the connection between interference and the Heisenberg uncertainty principle. A legacy of the famous discussions between Bohr and Einstein and highlighted by Feynman³¹ is that in obtaining the path information, we disturb the particle so that the interference pattern washes away. The new view is that interference disappears when the path information is present regardless of how it is obtained and regardless of whether that information is measured or not.³²

The third stage involves putting a polarizer along the X -direction after the interferometer. This polarizer is “the eraser” because it erases the path information. In this case we use the following matrix after the interferometer:

$$\hat{E} = \begin{pmatrix} 1/2 & 1/2 & 0 & 0 \\ 1/2 & 1/2 & 0 & 0 \\ 0 & 0 & 1 & 0 \\ 0 & 0 & 0 & 1 \end{pmatrix}, \quad (20)$$

where again we insert appropriate expressions in the 2×2 submatrices of the 4×4 matrix. In this case the matrix for

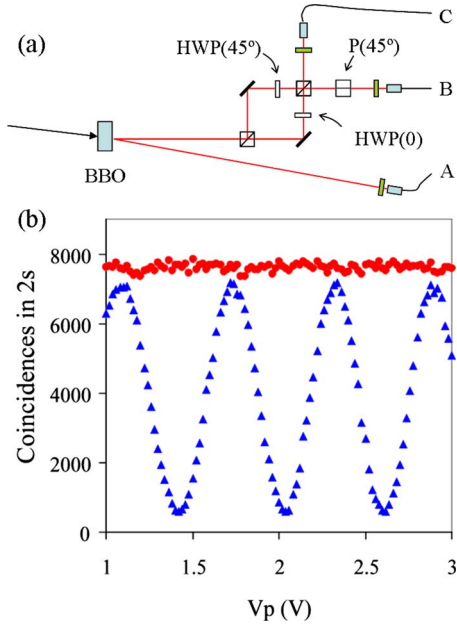


Fig. 3. Schematic of the (a) apparatus and (b) data for the quantum eraser. The data show cases when the light leaves the interferometer along the X direction not carrying path information (triangles) and when the light leaves along the Y direction carrying path information (circles).

the polarizer with its transmission axis 45° from the horizontal is placed in the diagonal submatrix corresponding to the X-direction, and the identity is placed in the submatrix corresponding to the Y propagation direction.

It is interesting that in recording the photon counts at both output ports of the interferometer, we obtain distinct results. This experimental condition was implemented with the setup shown in Fig. 3(a). Along the X-direction after the interferometer we had the eraser-polarizer, and along the Y-direction there was no polarizer. The non-normalized output for this case is

$$\hat{E}\hat{Z}_{dp}(\pi/4)|XV\rangle = \frac{i}{2} \begin{pmatrix} (e^{i\delta_1} - e^{i\delta_2})/2 \\ (e^{i\delta_1} - e^{i\delta_2})/2 \\ ie^{i\delta_1} \\ ie^{i\delta_2} \end{pmatrix}. \quad (21)$$

Along the X direction, which has the eraser-polarizer, the probability is

$$|(\hat{P}_X \otimes \hat{I})\hat{E}\hat{Z}(\pi/4)|XV\rangle|^2 = (1/4)(1 - \cos \delta), \quad (22)$$

and along the Y-direction where there is no polarizer, the probability is

$$|(\hat{P}_Y \otimes \hat{I})\hat{E}\hat{Z}(\pi/4)|XV\rangle|^2 = 1/2. \quad (23)$$

The experimental data is shown in Fig. 3(b). In the output where the path information was erased (X), we see interference in the coincidences at detectors A and B, as shown by the triangles. In the output where the light has distinguishing information (Y), we see no interference in the coincidences between detectors A and C, as shown by the circles. This experiment balances nicely the algebraic and the conceptual aspects of quantum mechanics.

A variation of this case is given by the polarization interferometer. In this case the symmetric nonpolarizing beam

splitter of a setup such as the one in Fig. 1 are replaced by polarizing beam splitters, which transmit the horizontally polarized light and reflect the vertically polarized light. The operator for the polarizing beam splitter \hat{B}_P is given by¹⁹

$$\hat{B}_P = \begin{pmatrix} 1 & 0 & 0 & 0 \\ 0 & 0 & 0 & 1 \\ 0 & 0 & 1 & 0 \\ 0 & 1 & 0 & 0 \end{pmatrix}. \quad (24)$$

Because there are no restrictions on the reflection phase, we choose zero for simplicity. The polarization interferometer is

$$\hat{Z}_P = \hat{B}_P(\hat{A} \otimes \hat{I})(\hat{M} \otimes \hat{I})\hat{B}_P. \quad (25)$$

For light to go through both arms of the interferometer, it must enter it having both components of the polarization. Thus, it must be in the initial state $|\psi_i\rangle = |X\rangle \otimes |D\rangle$, where

$$|D\rangle = (1/\sqrt{2}) \begin{pmatrix} 1 \\ 1 \end{pmatrix} \quad (26)$$

represents the state of the light with “diagonal” polarization, that is, it forms a 45° angle with the horizontal. It is easy to show that $|(\hat{P}_X \otimes \hat{I})\hat{Z}_P|\psi_i\rangle|^2 = 0$, that is, the light does not exit the interferometer along the X-direction. If we put a detector in the Y output, we find that there is no interference—all of the light goes out through the Y output. Polarization labels the paths so that they are distinguishable. If we put a polarizer after the Y output with the transmission axis making an angle of 45° with the horizontal (that is, transmitting state $|D\rangle$), it erases the distinguishing information and interference appears. The data before and after the polarizer is placed are similar to those of Fig. 3(b). Although this experiment is not part of our laboratory, we use it as a homework problem. A provocative question is the following: What is the polarization state of the photon as it goes through the interferometer? Undefined!

The polarizing beam splitter can also function as a controlled-not (CNOT) gate. In this gate the state of one qubit controls whether another qubit is left alone or NOT-ed. In this case the polarization is the control qubit, and the direction of propagation is the target qubit: When the polarization is horizontal, the direction of propagation remains the same, and when vertical, the direction of propagation flips. An interesting interference experiment related to this one uses the Jamin–Lebedeff interferometer in which calcite polarization beam displacers act as polarizing beam splitters.³³

With this basic arrangement we can prepare a photon in the state

$$|\psi\rangle = \frac{1}{\sqrt{2}}(|XH\rangle + |YV\rangle), \quad (27)$$

which is a nonseparable state of the two modes: An “entangled” state of modes of the same particle. This state violates the Bell inequalities¹⁵ and violates classical realism and noncontextuality but not nonlocality. Contextuality is a property of quantum mechanics whereby the state of a system depends on the context of previous measurements.

One final note for these experiments is that the quantum character of the experiments is retained by ensuring that photons are “heralded.” That is, that we detect their partners

produced by parametric down-conversion and record the data in coincidence. This procedure yields the light source “non-classical” because it obeys sub-Poissonian statistics (see next section).

B. Digression on the single-photon character of some of the experiments

Up to now all the results of the experiments can be reproduced with an attenuated source of light and a photomultiplier. If there is no need to demonstrate that photons exist, we can even do the low-cost quantum eraser with a double-slit-type experiment.³⁴ These experiments are very good at illustrating fundamental aspects of quantum mechanics, but they do not show that quantum mechanics is the correct approach to explain them. Thus, we ask: Why bother with such a complicated setup (down-conversion and coincidences)? The issue is that because a classical-wave description gives the same answer, we may get the impression that using a quantum mechanical description is unnecessary. If we were to do the experiments with electrons, this question would not arise because we mostly deal with electrons as whole particles, and spins underscore their quantum character more easily than an interference experiment. For light the classical-wave description goes a long way toward explaining most optical phenomena. We can modify the apparatus so that a classical-wave description is not appropriate. It involves performing a Hanbury–Brown–Twiss test.

We recommend several very illuminating descriptions of the Hanbury–Brown–Twiss experiment^{35,36} (see also Refs. 4 and 7). The Hanbury–Brown–Twiss test consists of adding a beam splitter after the interferometer (or all alone in the path of one of the down-converted photons^{4,37} or even at both outputs of the interferometer³⁸). We then measure photons at the output ports of the beam splitter and record the coincidences of those detections and the partner photon that goes directly to a detector. The predictions of the outcome of such a measurement are disparate: No coincidences for photons (photons are whole and do not split at a beam splitter) or coincidences for waves (waves split at a symmetric beam splitter). In our formalism this question is trivial because we are assuming a single quantum, and the outputs of the beam splitter have orthogonal eigenstates so that the probability of measuring a single quantum in both states is zero.

The simple-minded analysis of an attenuated source assumes that we have photons that enter the apparatus every once in a while. Do they? On the average, yes, but individually not always. If we use an attenuated beam, we will measure coincident detections at the outputs of the beam splitter because the photons arrive at random times and there is a nonzero probability that they come together and split at the beam splitter.³⁹ In photon-speak we say that the source mimics the predictions of classical waves because it follows Poisson statistics. However, the detection of the beam splitter outputs in coincidence with the heralding photon does not mimic classical waves because here we have a quantum process that produces pairs of photons, and the detection of one indicates the presence of the other one.⁴⁰ The occurrence of simultaneous production of identical pairs is very unlikely, and so coincidence detection yields photons that do not come in bunches (they are antibunched) and so follow sub-Poissonian statistics.⁴¹

The Hanbury–Brown–Twiss test involves measuring the second-order coherence coefficient $g_2(0) = N_{ABC}N_A / N_{AB}N_{AC}$,

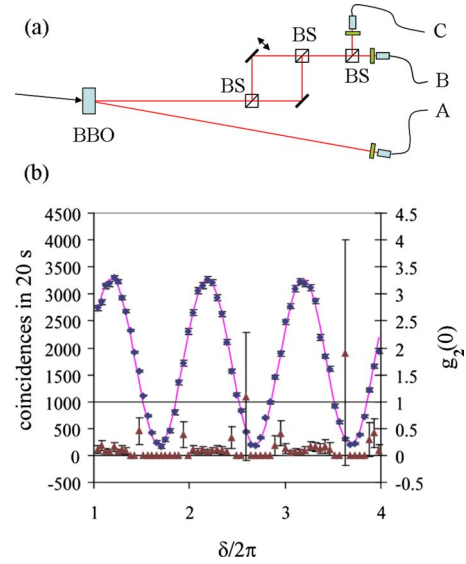


Fig. 4. Schematic of the (a) apparatus and (b) data for measuring outputs of single-photon interference. Coincidence at detectors *A* and *B* (circles; left scale) shows single-photon interference as a function of the interferometer phase. The solid line is a fit to the data with $a[1 + v \cos \delta(V_p)]$ and $\delta(V_p) = \alpha + \beta V_p + \gamma V_p^2$, where a , v , α , β , and γ are the fitting parameters. The calculated values of the second-order coherence coefficient $g_2(0)$ were obtained via the triple coincidences at detectors *A*, *B*, and *C* (triangles; right scale).

where *A*, *B*, and *C* label the detectors. The rationale of the test is that the quantum mechanics of photons predicts $g_2(0) = 0$ and classical-wave analysis predicts $g_2(0) \geq 1$. In essence the test is about the existence of the photon because it expects coincident detections at the same wavelength as the input to the beam splitter. It has been shown that $g_2(0)$ is connected to the photon statistics.⁴¹ The apparatus is shown in Fig. 4(a). In Fig. 4(b) we show the measurements of $g_2(0)$ for the experiment on single-photon interference. The circles show the coincidences N_{AB} between detectors *A* and *B* as a function of the interferometer phase. In this experiment we recorded the coincidences N_{AC} between *A* and *C*, which we do not show because they fall on top of the data for N_{AB} . We also recorded the triple coincidences N_{ABC} (or the coincidences in N_{AB} and N_{AC}), which we do not show because they are in single digits. The triangles in Fig. 4(b) show the calculated $g_2(0)$ as a function of the interferometer phase, with the scale on the right side of the graph. It is seen that all of the data are consistent with $g_2(0) < 1$.

For error bars we used \sqrt{N} , where N is the number of counts, and propagated it appropriately. We used these errors because it has been shown that detector inefficiencies can yield Poissonian variances.⁴¹ The two points with large error bars involved one triple-coincidence count, which led to final uncertainties that were greater than the magnitude of the data.

C. Two photons in direction-of-propagation modes

In this case both photons produced by parametric down-conversion enter the interferometer collinearly as shown in Fig. 5(a). The two-qubit states are given by the tensor product of the direction-of-propagation qubits of the two photons. If the eigenstates are given by $|X_1X_2\rangle$, $|X_1Y_2\rangle$, $|Y_1X_2\rangle$, and $|Y_1Y_2\rangle$, the two-qubit states are given by

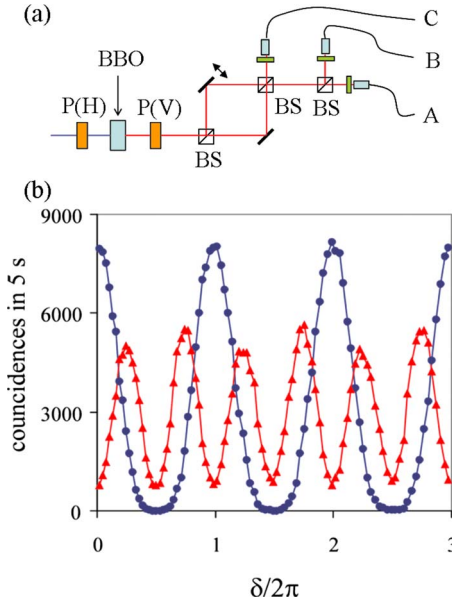


Fig. 5. Schematic of the (a) apparatus and (b) data for the experiment where both photons enter the interferometer collinearly. The data show cases where both photons are detected leaving the same port of the interferometer (circles; coincidences at detectors A and B) and separate ports of the interferometer (triangles; coincidences in detectors A and C).

$$|\psi\rangle = \begin{pmatrix} \langle X_1 X_2 | \psi \rangle \\ \langle X_1 Y_2 | \psi \rangle \\ \langle Y_1 X_2 | \psi \rangle \\ \langle Y_1 Y_2 | \psi \rangle \end{pmatrix}. \quad (28)$$

The interferometer operator with a nonpolarizing beam splitter is now given by

$$\hat{Z}_{dd} = (\hat{B} \otimes \hat{B})(\hat{A} \otimes \hat{A})(\hat{M} \otimes \hat{M})(\hat{B} \otimes \hat{B}). \quad (29)$$

Because photon pairs enter the interferometer collinearly, the initial state of the light is $|\psi_i\rangle = |X_1 X_2\rangle$. At this point the matrix algebra becomes laborious, and it is recommended that students use a software package that allows symbolic matrix manipulations. The output state is

$$\hat{Z}_{dd}|\psi_i\rangle = \frac{1}{4} \begin{pmatrix} -(e^{i\delta_1} + e^{i\delta_2})^2 \\ -i(e^{i2\delta_1} - e^{i2\delta_2}) \\ -i(e^{i2\delta_1} - e^{i2\delta_2}) \\ (e^{i\delta_1} - e^{i\delta_2})^2 \end{pmatrix}. \quad (30)$$

The probability of detecting both photons after the interferometer is

$$\mathcal{P}_{XX} = |\langle X_1 X_2 | \hat{Z}_{dd} |\psi_i\rangle|^2 = (1/4)(1 + \cos \delta)^2. \quad (31)$$

In the laboratory we recorded data for this possibility by measuring the coincidences from detectors A and B [see Fig. 5(a)]. The data for this case (circles in Fig. 5(b)), with sharp maxima and flat minima, are consistent with the prediction of Eq. (31).

The probability of detecting photons exiting through separate ports of the interferometer is

$$\mathcal{P}_{XY} = |\langle \psi_{XY} | \hat{Z}_{dd} |\psi_i\rangle|^2 = (1/4)(1 - \cos 2\delta), \quad (32)$$

where

$$|\psi_{XY}\rangle = \frac{1}{\sqrt{2}}(|X_1 Y_2\rangle + |Y_1 X_2\rangle). \quad (33)$$

The latter is a wave function consistent with the bosonic nature of light: It must be symmetric under the exchange of the particle labels. The data for this case were obtained by recording the coincidences from detectors A and C in Fig. 5(a). As can be seen in Fig. 5(b), the data (triangles) show fringes that are twice the frequency of single-photon interference, consistent with Eq. (32). The striking result is that the interference pattern has twice the frequency of the single-photon interference pattern. Nonclassical interference shows new quantum aspects: two photons acting as a single quantum object (a biphoton).

In the apparatus of Fig. 5(a) the crystal was tilted for collinear down-conversion. Because down-converted photons are orthogonal to the photons incident to the crystal (pump photons), we stop the pump photons from going further in the apparatus by placing crossed Glan-Thompson polarizers before and after the beta-barium-borate crystal. They also stop an infrared output of the laser that cannot be blocked easily with filters. We note that this experiment is possibly the most challenging one because the shape of the fringes in the data for photons leaving separate ports of the interferometer relies on identical symmetric beam splitters and the alignment of the interferometer. The straight-through fringes are more robust and do not depend on whether the two beam splitters are identical or not.

We note that the output of the Hong-Ou-Mandel interference⁴²—two indistinguishable photons reaching a beam splitter from X and Y input ports—is given by $(\hat{B} \otimes \hat{B})|\psi_{XY}\rangle = (i/\sqrt{2})(|X_1 X_2\rangle + |Y_1 Y_2\rangle)$. That is, when the two photons are indistinguishable, they come along the same output port, which experimentally results in a “dip” in the coincidences. The biphoton interferometer is a variation of the Hong-Ou-Mandel interference for which we obtain fringes instead of a single dip.

D. Two photons in polarization modes

This case has been studied widely because it leads to violations of Bell’s inequalities. Introducing students to this problem touches a fundamental aspect of physics: realism and nonlocality. Students perform a test that dispels a misconception: Confusing entangled states with mixed states. Each particle has a polarization qubit so that the states are described by four-dimensional two-qubit vectors. For example, the noncollinear entangled state produced by the two-crystal source,^{2,43} where the light is in a superposition of both photons in the horizontal polarization state and both photons in the vertical polarization state, is given by

$$|\psi\rangle = \frac{1}{\sqrt{2}}(|H_1 H_2\rangle + |V_1 V_2\rangle). \quad (34)$$

This state exhibits nonclassical properties that are at the heart of quantum mechanics. The polarization state of either photon is undefined until we make a measurement. This view is contrary to a realistic one, where half the time the photons are in state $|H_1 H_2\rangle$ and the other half in state $|V_1 V_2\rangle$. Besides doing an experimental measurement that violates Bell inequalities,^{3,44} there is an experimental test that we can perform to distinguish between entangled and mixed states. However, the simple ket notation is not convenient to repre-

sent the mixed state. Here we must introduce students to a quantum mechanical tool that is much forgotten in quantum mechanics texts: The density matrix.

For the pure state of Eq. (34) the density matrix is given by^{21,45}

$$\rho_\psi = |\psi\rangle\langle\psi| = \frac{1}{2} \begin{pmatrix} 1 & 0 & 0 & 1 \\ 0 & 0 & 0 & 0 \\ 0 & 0 & 0 & 0 \\ 1 & 0 & 0 & 1 \end{pmatrix}. \quad (35)$$

The density matrix for the mixed state referred to previously is given by⁴⁵

$$\begin{aligned} \rho_{\text{mixed}} &= \frac{1}{2} |H_1 H_2\rangle\langle H_1 H_2| + \frac{1}{2} |V_1 V_2\rangle\langle V_1 V_2| \\ &= \frac{1}{2} \begin{pmatrix} 1 & 0 & 0 & 0 \\ 0 & 0 & 0 & 0 \\ 0 & 0 & 0 & 0 \\ 0 & 0 & 0 & 1 \end{pmatrix}. \end{aligned} \quad (36)$$

The difference between the pure and mixed states is evident when comparing the matrices in Eqs. (35) and (36): The density matrix for the mixed state does not have off-diagonal elements.⁴⁵ There are two more concepts that are necessary in using this formalism. When we do a measurement, we collapse the system described by ρ onto the eigenstate of the measuring device, say, $|\phi\rangle$ with density matrix ρ_ϕ . The probability of the outcome is the trace of the product of the two density matrices: $\mathcal{P} = \text{Tr}(\rho_\phi \rho)$. If the state is processed by a device represented by the operator, say, \hat{R} , the density matrix transforms into $\hat{R} \rho \hat{R}^\dagger$, where \hat{R}^\dagger is the adjoint of \hat{R} .

The experiment to distinguish between mixed and entangled states consists of preparing photons in the entangled state given by Eq. (34). The pump photons leave the source horizontally polarized. A half-wave plate rotates the polarization of the pump light to be at 45° with the horizontal. The two components of the pump are predephased by a wave plate and sent to a two-crystal stack of rotated type-I 0.5 mm thick down-conversion crystals.^{2,43} (The birefringence of the crystals inserts a phase between the two product states of Eq. (34) such that the predephasing of the pump components is adjusted so that the phase after the crystals is zero.) An alternate method uses two crystals, one in the path of each down-converted photon.^{46,47} The phase matching angle of the crystal was adjusted for down-converted photons, leaving the crystals at angles of $\pm 3^\circ$ relative to the pump beam axis to spatially separate the path of the two photons (see Fig. 6).

The experiment is designed to have polarizers in the paths of the down-converted photons. One polarizer is set to 45° and the other one is rotated. We then record the coincidences as a function of the angle of the rotated polarizer. The polarizers project the entangled state of the light onto the state

$$|\phi\rangle = \begin{pmatrix} \cos \alpha \\ \sin \alpha \end{pmatrix} \otimes \frac{1}{\sqrt{2}} \begin{pmatrix} 1 \\ 1 \end{pmatrix} = \frac{1}{\sqrt{2}} \begin{pmatrix} \cos \alpha \\ \cos \alpha \\ \sin \alpha \\ \sin \alpha \end{pmatrix}. \quad (37)$$

The probability of detecting the light depends on the initial state. If it is the pure state, we obtain $\text{Tr}(\rho_\phi \rho_\psi)$

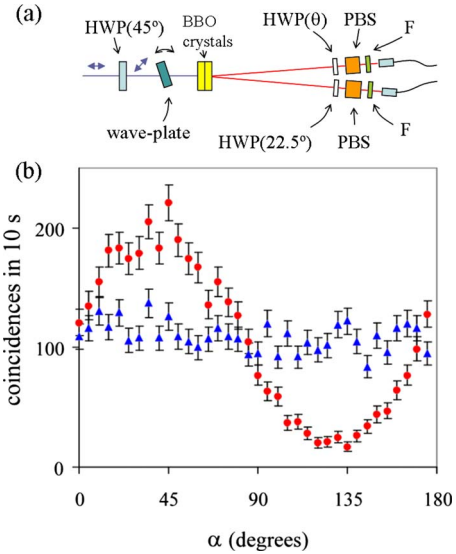


Fig. 6. Schematic of the (a) apparatus and (b) data for the experiment showing the correlations of photon pairs in maximally entangled states (circles) compared to mixed states (triangles).

$= (1/4)(1 + \sin 2\alpha)$, and if it is in the mixed state, we obtain $\text{Tr}(\rho_\phi \rho_{\text{mixed}}) = (1/4)$, a clear difference between the two explanations.

An experimental detail is that because near-infrared polarizers are difficult to come by, it is more practical to have polarizing beam splitters. These may be rotated provided they are properly mounted. An alternative is to keep them fixed and put half-wave plates before them. The action of the half-wave plates and fixed polarizing beam splitters can also be included in the algebraic manipulations, which is how the data of Fig. 6(b) were obtained. The horizontal axis is $\alpha = 2\theta$, with θ being the angle of the half-wave plate in front of the polarizer for the photon labeled 1. These data are consistent with the expected quantum mechanical correlations.

We mimicked the mixed state by putting a polarizer before the crystal and taking data for half the time with the pump beam polarized vertically and half the time with the pump beam horizontally. The two data sets were then added together to produce the data shown by the triangles in Fig. 6(b). As can be seen, the data show no correlations, consistent with the expectation for a mixed state.

If we place a half-wave plate in the path of one of the beams, we can change these results. If the fast axis of the wave plate is set to be vertical, the polarization state of the light changes to $|\chi\rangle = (1/\sqrt{2})(|H_1 H_2\rangle - |V_1 V_2\rangle)$. This problem can be done algebraically by constructing the operator for the wave plate in one arm and nothing on the other arm: $\hat{R} = (\hat{W}_{\lambda/2}(0) \otimes \hat{I})$, and then verifying that it converts state $|\psi\rangle$ into state $|\chi\rangle$ (that is, by showing $\rho_\chi = \hat{R} \rho_\psi \hat{R}^\dagger$). In this case the correlations change, and we can show that $\text{Tr}(\rho_\phi \rho_\chi) = (1/4) \times (1 - \sin \alpha)$; the result for the mixed state remains the same, as shown in Fig. 6. For an entangled state, actions on one particle affect the other one via their entangled state.

IV. HIGHER QUBIT SPACES

We have described situations involving combinations of three different modes: Polarization, direction of propagation,

and particle number. If we combine all three modes, we obtain higher qubit spaces. The formalism presented here is also appropriate to describe other experiments. If we use entanglement to specify path information^{13,14} (that is, a non-local form of the eraser), we have three qubits. If we “hyper-entangle” the photons in polarization, direction of propagation, and particle number in an experiment such as the polarization form of the Hong–Ou–Mandel experiment, we have four qubits and a 16-dimensional space.^{48–50} In these experiments the indistinguishability of the two photons creates the interference. It can be manipulated via operations on the polarization of the light so as to produce no coincidences (the famous Hong–Ou–Mandel dip) or a peak in coincidences. Other possibilities involve the use of spatial modes, but these are beyond the scope of these undergraduate laboratories.

V. THE LABORATORY

In our laboratory section we had two setups. Both shared the four-detector module, but each setup had its own optical breadboard, pump diode laser, electronics, and personal computer. The previous time that the laboratory was offered, the setups shared the pump laser, and the light was split by a beam splitter and directed to the two setups, which were laid out on two end-adjacent optical breadboards. In the 2009 Spring semester, groups of three students worked on an individual setup. We had four groups, and therefore each student did a laboratory every other week. Because the laboratory sessions were limited to one afternoon, the setups were all aligned before the laboratory, and students did only modest modifications to the setups, which did not involve realignment of the detectors or interferometers. In laboratories with longer time periods, students can be assigned to align the apparatus.

The laboratory write-ups had questions for extensive post-laboratory analysis. These questions involved doing matrix manipulations such as the ones described in this article. Students were asked to compare theory and experiments by graphing the data and theory deduced from their analysis. There were also some conceptual questions. The write-ups gave students some freedom to avoid a cookbook approach, although the main thrust of the experiment was preordained. Laboratory reports were individual, but students were encouraged to work together.

The laboratory was optional for students; 12 chose to take it and nine chose not. A first indicator of the outcome is the class grade. The students that took the laboratory had a combined final class grade of $88 \pm 12\%$, while the students who did not take the laboratory had a final grade of $75 \pm 13\%$. The uncertainties are the standard deviations of the final grades. The averages are a full letter-grade apart, which is significant. Because of the dual population, the class was taught as if students were not taking the laboratory. The result is that the laboratory did add to their understanding of the subject, as reflected in the grades. However, those doing the laboratory put more time and effort as a consequence of doing the laboratory exercises.

Postlaboratory assessments via an anonymous questionnaire with multiple-choice and open-ended questions were very positive. The numerical portion (with possible answers: 1=strongly disagree, 2=disagree, 3=neutral, 4=agree, and 5=strongly agree) involved directed questions. A sample of the questions and ratings include “The quantum labs helped

me understand the concept of superposition in quantum mechanics:” 4.7; “Experiments showed that quantum effects are real:” 4.9; “The labs showed how the different formulations (e.g., matrix and state-vector) are applied to a real situation:” 4.6; “By taking the lab I understood class better:” 4.7; and “If I were to do it again I would take the lab:” 5. Students were encouraged to add comments. They commented about how working out the theory for the experiment gave the algebra some meaning and a sense of purpose to the theory. However, they still remarked how striking they found the whole experience in the sense of doing an experiment that is explained by theory but that conceptually was still puzzling. The answer to the following question was surprising: “Colgate University should require students to take both the lecture and lab part:” 3.2. Apparently Colgate students resent being forced to take required components. Students found the quantum eraser more striking than the experiment on entanglement. Perhaps that is a measure of their lack of experience with classical optics, as those who have that experience (that is, faculty) find the nonclassical entanglement experiments more striking. Or perhaps, their surprise is a more unbiased reaction at superposition, “the only mystery of quantum mechanics” as said by Richard Feynman.³¹

In summary, I have presented a matrix-based formalism for using correlated-photon experiments for teaching a laboratory component of quantum mechanics. This formalism worked well for explaining the experiments in the language of the quantum mechanics course. It also served to introduce aspects of the emerging field of quantum information.

ACKNOWLEDGMENTS

The author would like to thank Paul Alsing, Mark Beck, Francisco De Zela, Reinhard Erdmann, Mike Fanto, and Richard Michalak for very useful discussions and interactions and Michael Chang for laboratory assistance. This work was funded by National Science Foundation under Grant No. DUE-042882.

¹C. H. Holbrow, E. J. Galvez, and M. E. Parks, “Photon quantum mechanics and beam splitters,” *Am. J. Phys.* **70**, 260–265 (2002).

²D. Dehlinger and M. W. Mitchell, “Entangled photon apparatus for the undergraduate laboratory,” *Am. J. Phys.* **70**, 898–902 (2002).

³D. Dehlinger and M. W. Mitchell, “Entangled photons, nonlocality, and Bell inequalities in the undergraduate laboratory,” *Am. J. Phys.* **70**, 903–910 (2002).

⁴J. J. Thorn, M. S. Neel, V. W. Donato, G. S. Bergreen, R. E. Davies, and M. Beck, “Observing the quantum behavior of light in an undergraduate laboratory,” *Am. J. Phys.* **72**, 1210–1219 (2004).

⁵E. J. Galvez, C. H. Holbrow, M. J. Pysher, J. W. Martin, N. Courtemanche, L. Heilig, and J. Spencer, “Interference with correlated photons: Five quantum mechanics experiments for undergraduates,” *Am. J. Phys.* **73**, 127–140 (2005).

⁶Correlated-photon experiments have been implemented in the advanced laboratory at Harvey Mudd College R. Haskell (private communication, 2009).

⁷See the article by B. J. Pearson and D. P. Jackson in this volume on adapting these experiments for use in the second-year modern physics laboratory.

⁸Three weeks of lecture and an experiment on the quantum eraser are offered in Colgate University’s first-semester course on quantum physics. This approach will appear in C. H. Holbrow, J. N. Lloyd, J. C. Amato, E. J. Galvez, and M. E. Parks, *Modern Introductory Physics*, 2nd ed. (Springer-Verlag, New York, 1999).

⁹Other creative approaches include a web-based lab. See P. Bronner, A. Strunz, C. Silberhorn, and J.-P. Meyn, “Interactive screen experiments with single photons,” *Eur. J. Phys.* **30**, 345–353 (2009) and

- www.didaktik.physik.uni-erlangen.de/quantumlab/english/).
- ¹⁰ See: departments.colgate.edu/pql.htm.
- ¹¹ See: people.whitman.edu/~beckmk/QM/.
- ¹² See: www.optics.rochester.edu/workgroups/lukishova/QuantumOpticsLab/.
- ¹³ M. J. Pysher, E. J. Galvez, K. Misra, K. R. Wilson, B. C. Melius, and M. Malik, "Nonlocal labeling of paths in a single-photon interferometer," *Phys. Rev. A* **72**, 052327 (2005).
- ¹⁴ E. J. Galvez, M. Malik, and B. C. Melius, "Phase shifting of an interferometer using nonlocal quantum-state correlations," *Phys. Rev. A* **75**, 020302 (2007).
- ¹⁵ B. R. Gadway, E. J. Galvez, and F. De Zela, "Bell-inequality violations with single photons in momentum and polarization," *J. Phys. B* **42**, 015503 (2009).
- ¹⁶ We found the following text particularly appropriate for this purpose: J. S. Townsend, *A Modern Approach to Quantum Mechanics* (University Science Books, Sausalito, 2000).
- ¹⁷ A. P. French and E. F. Taylor, *Introduction to Quantum Physics* (Norton, New York, 1978).
- ¹⁸ R. Blümel, *Foundations of Quantum Mechanics—From Photons to Quantum Computers* (Jones and Bartlett, Sudbury, 2010).
- ¹⁹ G. Chen, D. A. Church, B.-G. Englert, C. Henkel, B. Rohwedder, M. O. Scully, and M. Zubairy, *Quantum Computing Devices: Principles, Designs and Analysis* (Chapman and Hall/CRC, Boca Raton, 2007).
- ²⁰ S. Loepp and W. K. Wothers, *Protecting Information: From Classical Error Correction to Quantum Cryptography* (Cambridge U. P., Cambridge, 2006).
- ²¹ M. A. Nielsen and I. L. Chuang, *Quantum Computation and Quantum Information* (Cambridge U. P., Cambridge, 2000).
- ²² N. D. Mermin, *Quantum Computer Science: An Introduction* (Cambridge U. P., Cambridge, 2007).
- ²³ N. S. Yanofsky and M. A. Mannucci, *Quantum Computing for Computer Scientists* (Cambridge U. P., Cambridge, 2008).
- ²⁴ M. Hirvensalo, *Quantum Computing* (Springer-Verlag, Berlin, 2004).
- ²⁵ C. W. Misner, K. S. Thorne, and W. H. Zurek, "John Wheeler, relativity, and quantum information," *Phys. Today* **62** (4), 40–46 (2009).
- ²⁶ E. Hecht, *Optics* (Addison-Wesley, Reading, MA, 2002).
- ²⁷ B.-G. Englert, C. Kurtsiefer, and H. Weinfurter, "Universal unitary gate for single-photon two-qubit states," *Phys. Rev. A* **63**, 032303 (2001).
- ²⁸ E. J. Galvez, "Gaussian beams in the optics course," *Am. J. Phys.* **74**, 355–361 (2006).
- ²⁹ D. Branning, S. Bhandari, and M. Beck, "Low-cost coincidence-counting electronics for undergraduate quantum optics," *Am. J. Phys.* **77**, 667–670 (2009).
- ³⁰ J. W. Lord, "Coincidence counting using a field programmable gate array (FPGA)," Honors thesis, Whitman College, Walla, Walla, WA (2008); available in Ref. 11.
- ³¹ R. P. Feynman, R. B. Leighton, and M. Sands, *The Feynman Lectures on Physics* (Addison-Wesley, Reading, MA, 1965), Vol. 3, pp. 1-1.
- ³² M. O. Scully, B.-G. Englert, and H. Walther, "Quantum optical tests of complementarity," *Nature (London)* **351**, 111–116 (1991).
- ³³ A. Gogo, W. D. Snyder, and M. Beck, "Comparing quantum and classical correlations in a quantum eraser," *Phys. Rev. A* **71**, 052103 (2005).
- ³⁴ R. Hillmer and P. G. Kwiat, "A do-it-yourself quantum eraser," *Sci. Am.* **296** (5), 90–95 (2007).
- ³⁵ G. S. Greenstein and A. G. Zajonc, *The Quantum Challenge: Modern Research on the Foundations of Quantum Mechanics* (Jones and Bartlett Publishers, Boston, 2005).
- ³⁶ M. Fox, *Quantum Optics* (Oxford U. P., Oxford, 2006).
- ³⁷ P. Grangier, G. Roger, and A. Aspect, "Experimental evidence for a photon anticorrelation effect on a beam splitter: A new light on single-photon interferences," *Europhys. Lett.* **1**, 173–179 (1986).
- ³⁸ E. J. Galvez and M. Beck, "Quantum optics experiments with single photons for undergraduate laboratories," in *Education and Training in Optics 2007*, edited by M. Nantel (Ontario Centres of Excellence, Ottawa, 2007), (spie.org/etop/etop2007.html).
- ³⁹ M. Beck, "Comparing measurements of $g(2)(0)$ performed with different coincidence detection techniques," *J. Opt. Soc. Am. B* **24**, 2972–2978 (2007).
- ⁴⁰ A. B. U'Ren, C. Silberhorn, J. L. Ball, K. Banaszek, and I. A. Walmsley, "Characterization of the nonclassical nature of conditionally prepared single photons," *Phys. Rev. A* **72**, 021802 (2005).
- ⁴¹ M. C. Teich and B. E. A. Saleh, in *Progress in Optics*, edited by E. Wolf (Elsevier, Amsterdam, 1988), Vol. 26, pp. 1–104.
- ⁴² C. K. Hong, Z. Y. Ou, and L. Mandel, "Measurement of subpicosecond time intervals between two photons by interference," *Phys. Rev. Lett.* **59**, 2044–2046 (1987).
- ⁴³ P. G. Kwiat, E. Waks, A. G. White, I. Appelbaum, and P. H. Eberhard, "Ultrabright source of polarization-entangled photons," *Phys. Rev. A* **60**, R773–R776 (1999).
- ⁴⁴ J. A. Carlson, D. M. Olmstead, and M. Beck, "Quantum mysteries tested: An experiment implementing Hardy's test of local realism," *Am. J. Phys.* **74**, 180–186 (2006).
- ⁴⁵ K. Blum, *Density Matrix Theory and Applications* (Plenum, New York, 1981).
- ⁴⁶ J. B. Altepeter, E. R. Jeffrey, and P. G. Kwiat, "Phase-compensated ultra-bright source of entangled photons," *Opt. Express* **13**, 8951–8959 (2005).
- ⁴⁷ G. M. Akselrod, J. B. Altepeter, E. R. Jeffrey, and P. G. Kwiat, "Phase-compensated ultra-bright source of entangled photons: erratum," *Opt. Express* **15**, 5260–5261 (2007).
- ⁴⁸ P. G. Kwiat, A. M. Steinberg, and R. Y. Chiao, "Observation of a 'quantum eraser': A revival of coherence in a two-photon interference experiment," *Phys. Rev. A* **45**, 7729–7739 (1992).
- ⁴⁹ A. V. Sergienko, Y. H. Shih, and M. H. Rubin, "Experimental evaluation of a two-photon wave packet in type-II parametric downconversion," *J. Opt. Soc. Am. B* **12**, 859–862 (1995).
- ⁵⁰ W. P. Grice, R. Erdmann, I. A. Walmsley, and D. Branning, "Spectral distinguishability in ultrafast parametric down-conversion," *Phys. Rev. A* **57**, R2289–R2292 (1998).